Calculated Bond Energies of Gas-Phase, Main-Group Metal Ions with Small Hydrocarbon Radicals

Simon Petrie[†]

School of Chemistry, University College, University of New South Wales, ADFA, Canberra, ACT 2600 Australia, and Department of Chemistry, the Faculties, Australian National University, Canberra, ACT 0200 Australia

Received: February 14, 2002

High-level ab initio calculations, using the CPd-G2thaw and CP-G2 composite computational procedures (combined with spin projection techniques when appropriate), are used to explore the bonding between the metal monocations Na^+, Mg^+, Al^+, K^+, and Ca^+ and the radicals H, CH_3, C_2H, C_2H_3, and C_2H_5. Assessment of existing and novel computational techniques for the second-row-metal-containing species finds significantly improved performance, as ascertained by residual basis set superposition error (BSSE) values, of the new variants over standard methods, and general recommendations for calculations on second-row-metal-containing ions are established. In sharp contrast to the results obtained from many studies of bonding between metal ions and closed-shell ligands, wide variations are seen for any given radical ligand among the bond strengths of different metal ions within a given row: for example, the Na^+-H bond strength is only 4.2 kJ mol^{-1} while the Mg^+-H bond strength (in the singlet state adduct) is 196.3 kJ mol^{-1}. Discrepancies between theoretical and literature experimental thermochemical values for MgH^+ and Mg_2H^+ contrast with generally very good agreement with previous studies for other species, suggesting that the energetics of MgH^+ and Mg_2H^+ may warrant further experimental study. Finally, the very large singlet-state adduct bond energies for Mg- and Ca-containing ions, and the notably small bond energies for Na- and K-containing adducts, suggest that radicals such as H and CH_3, encountered in environments such as jovian planetary atmospheres, outflowing circumstellar envelopes, and interstellar clouds, will display a high selectivity in their propensity to react with ambient metal ions.

1. Introduction

Very few data exist regarding the reactivity of metal ions with molecular radicals. This reflects the considerable experimental difficulties that beset this topic but belies the potential importance of such reactions in the chemistry of atmospheres. Metal-ion production from meteoritic ablation is held to be responsible for the occurrence of "sporadic-E" layer formation, in Earth's ionosphere[1−6] as well as those of other planets,[7−15] while monocations of the cosmically abundant metals (prototypically Na, Mg, and Fe) have also long been considered[16,17] as major carriers of positive charge within cold and comparatively dense gaseous astrophysical environments such as interstellar clouds and outflowing circumstellar envelopes. In all of these diverse environments, it is the apparent paucity of loss processes that is held responsible for the longevity of the atomic metal ions, for which the most straightforward neutralization process, viz., radiative recombination

$$M^+ + e \rightarrow M + h\nu \qquad (1)$$

is rather inefficient. Radiative association of M^+ with an appropriate ligand species X

$$M^+ + X \rightarrow MX^+ + h\nu \qquad (2)$$

can considerably hasten the removal of metal ions,[18] by providing an additional subsequent neutralization pathway of dissociative recombination

$$MX^+ + e \rightarrow M + X \qquad (3)$$

for which the recombination coefficient often exceeds that for process (1) by several orders of magnitude. Reactions of type (2) therefore play a crucial role in mitigating the degree of ionization within gas-phase environments.[19] Such reactions are also believed to account[20−23] for the formation of the metal cyanide radicals MgCN,[24] MgNC,[25] AlNC[26] and SiCN[27] that have been detected in the outflowing material from several mass-losing stars.

Within the upper atmospheric and extraterrestrial environments where the reaction chemistry of metal ions is of interest, hydrocarbon radicals often constitute an abundant class of potential reactants: H, C_2H, and C_4H in dense interstellar clouds and C-rich circumstellar envelopes;[16,17] H, CH_3, and C_2H_5 in the upper atmospheres of the Jovian planets;[28−32] and H, CH_3, C_2H, and C_2H_5 in the ionosphere of the Saturnian satellite Titan.[33−36] An understanding of the interactions of M^+ with hydrocarbon radicals thus has the potential to further our knowledge of the chemical evolution of such environments, and this is one focus of the present study.

A considerable number of previous ab initio studies have investigated the structural and thermochemical characteristics of NaH^+,[37−43] MgH^+,[37,42,44−53] and AlH^+.[37,42,54−63] Protonated forms of K[38,39,43] and Ca[46,47,50,64−69] have received rather less attention, and of the polyatomic ions investigated here only

[†] Present address: Department of Chemistry, the Faculties, Australian National University. E-mail: spetrie@rsc.anu.edu.au.

10.1021/jp020433j CCC: $22.00
Published on Web 04/19/2002

TABLE 1: Counterpoise Corrections for $MCCH^+$ Metal−Ligand Bond Energies

species	method[a]	$\delta(M^+)$[b] (mHartree)	$\delta(CCH)$[c] (mHartree)	CP_{to}[d] (kJ mol^{-1})	% BE[e]
$NaCCH^+$	MP2/6-311+G(3df,2p)	1.24	0.67	5.0	9.9
	MP2/dB4G	0.39	0.71	2.8	6.1
	QCISD(T)/dB4G	0.41	0.73	3.0	6.1
$^1MgCCH^+$	MP2/6-311+G(3df,2p)	1.88	0.85	7.1	2.0
	MP2/dB4G	0.80	0.87	4.4	1.2
	QCISD(T)/dB4G	0.86	0.89	4.6	1.3
$^3MgCCH^+$	MP2/6-311+G(3df,2p)	0.85	0.73	4.2	5.6
	MP2/dB4G	0.48	0.75	3.2	4.4
	QCISD(T)/dB4G	0.52	0.80	3.4	4.6
$AlCCH^+$	MP2/6-311+G(3df,2p)	1.89	0.83	7.1	3.0
	MP2/dB4G	1.18	0.83	5.3	2.3
	QCISD(T)/dB4G	1.03	0.87	5.0	2.1
$KCCH^+$	MP2/6-311+G(3df,2p)	0.16	0.24	1.1	3.5
	QCISD(T)/6-311+G(3df,2p)	0.18	0.26	1.2	3.8
$^1CaCCH^+$	MP2/6-311+G(3df,2p)	0.90	0.39	3.4	0.85
	QCISD(T)/6-311+G(3df,2p)	1.09	0.41	3.9	1.0
$^3CaCCH^+$	MP2/6-311+G(3df,2p)	0.63	0.29	2.4	3.0
	QCISD(T)/6-311+G(3df,2p)	0.77	0.31	2.8	3.5

[a] Level of theory employed in single-point geometry-corrected counterpoise correction calculations. The dB4G basis set for Na, Mg, and Al is as defined in the text. [b] Metal-ion contribution to the counterpoise correction; 1 mHartree = 2.6255 kJ mol^{-1}. [c] Ligand contribution to the counterpoise correction. [d] Total geometry-corrected counterpoise correction, obtained using the indicated level of theory. [e] Percent reduction in metal ion/ligand bond energy (ZPE included) on application of the counterpoise correction, using second-row G2thaw or third-row G2 (MP2/6-311+G(3df,2p)), d-G2thaw (MP2/dB4G), d-G2thaw(QCI) (QCISD(T)/dB4G), or third-row G2 (QCISD(T)/6-311+G(3df,2p)) values for the bond energy.

MCH_3^+ (M = Na, Mg, Al, Ca),[70−77] $MgCCH^+$,[53] and $Mg(C_2H_5)^+$ [78] have been previously described. Experimental results appear to exist only for the protonated metal atoms and for $MgCH_3^+$ [79] and $AlCH_3^+$.[73]

2. Theoretical Methods

Accurate description of both metal ions and molecular radicals in quantum chemical calculations requires a consideration of the potentially significant sources of error in standard calculations on such entities. In the case of main-group metal ions, most notably sodium, the poor agreement between otherwise highly reliable "model chemistry" approaches such as CBS-Q and G3 has been noted previously,[80] and recent studies have underlined the importance of choosing an appropriate correlation space (so as to include the outermost shell of "core" electrons in the metal atom),[69,81−86] correcting for basis set superposition error (BSSE),[87−90] and using basis sets designed to minimize the BSSE (since existing methods for BSSE correction are only approximate)[87,90,91] in calculations on alkali metal ion/ligand binding energies. We have extended the CPd-G2thaw approach, originally developed for calculations on Na-containing species,[90] to apply also to the Mg- and Al-containing molecular ions investigated herein. The CPd-G2thaw method,[90] broadly modeled on the G2 composite procedure,[92] involves the use of a modified 6-311+G(3df) basis set for the metal atom in some of the constituent calculations, by decontracting the second set of contracted s functions, and the second set of contracted p functions of the standard[93] 6-311+G(3df) basis set. A full description of the CPd-G2thaw method (for sodium) has been reported previously,[90] and calculations involving Mg and Al are performed in an entirely analogous fashion. For K and Ca, the basis sets and correlation space defined for the standard G2 method are generally appropriate (test calculations involving a decontracted 6-311+G(3df) basis for potassium, in several K-containing adduct ions, show very little improvement in BSSE when assessed against calculations using the standard 6-311+G(3df) basis; this is in marked contrast to the very large improvement seen for Na-containing ions[90] upon similar basis set decontraction) and so we have opted to use the G2 method for K- and Ca-containing species,[69] modified only by application of a counterpoise correction for BSSE that is calculated at the MP2(thaw)/6-311+G(3df) level of theory.

To assess the performance of CPd-G2thhaw for Mg and Al, and to test the validity of the assumption[89,90] that the MP2(thaw) counterpoise correction is a very close approximation to the counterpoise correction obtained at the QCISD(T)(thaw) level of theory that CPd-G2thaw is intended to emulate, we have determined the counterpoise corrections for the $MCCH^+$ ions at several levels of theory. These values, displayed in Table 1, show (first) that partial decontraction of the 6-311+G(3df) basis set for Mg and Al leads to a significant reduction (albeit less dramatic than that seen for sodium)[90] in the magnitude of the metal-ion component of the counterpoise correction and (second) that the MP2(thaw) counterpoise correction is always between 85% and 115% of the corresponding QCISD(T)(thaw) value. The first of these observations validates our use of the partially decontracted Mg and Al basis sets in calculations on adducts of these metal ions, while the second justifies the use[89] of the much more economical MP2(thaw) level, rather than QCISD(T)(thaw), in determination of the counterpoise correction (which is always, in any event, only an approximation to the true basis set superposition error). Note, also, that the ligand component of the counterpoise correction is much larger for the second-row, than for the third-row, metal-ion adducts, presumably reflecting the larger M^+/CCH separations (and therefore reduced opportunity for basis set superposition) in the third-row-containing species.

Problems in computations on molecular radicals are most often associated with spin contamination by states of other multiplicity. To address this problem, we have evaluated the binding energies for metal-ion adducts using the approximate projected second- and fourth-order Møller−Plesset single-point energies, in place of the analogous unrestricted energies, in the G2-type composite procedure. This approach has previously been adopted in calculations on open-shell Na-, Mg-, and Al-containing species.[94−97] However, its general reliability has not been established, and so it is difficult to judge its validity for the species in question here. An alternative approach is to use a "model chemistry" specifically designed to correct for the effect of spin contamination, and we have thus used the CBS-

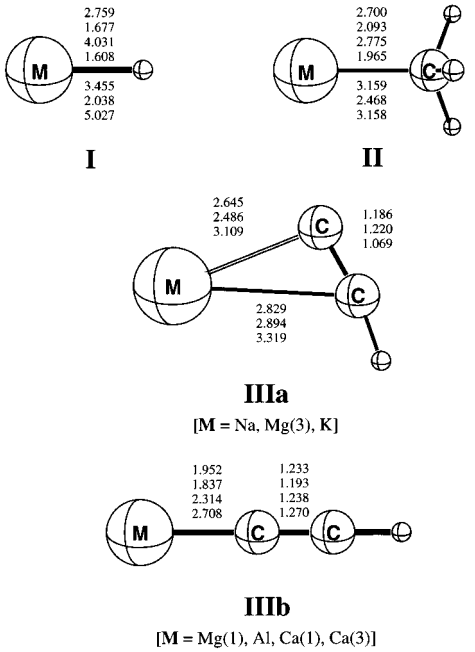

Figure 1. MP2(full)/6-31G* optimized geometries for MH^+, MCH_3^+, and $MCCH^+$. Bond lengths between heavy atoms are shown in Ångstroms. Except where otherwise noted, parameters listed in order are for adducts of Na^+, Mg^+ (singlet, followed by triplet, adduct), Al^+, K^+, and Ca^+ (singlet, then triplet).

RAD method recommended by Radom and co-workers[98] in calculations on the Al-containing adducts.[99]

All calculations were performed using the GAUSSIAN98 suite of quantum chemical programs.[100]

3. Results and Discussion

3.1. General Structural and Energetic Trends. Optimized geometries for the adduct ions are summarized in Figures 1 and 2, while bonding energies are given in Table 2.

Several trends can be discerned in these results. First, for each ligand X the M^+-X bond strengths essentially follow the rule (Mg^+, Ca^+ (singlet adducts)) > (Al^+) > (Mg^+, Ca^+ (triplet adducts), Na^+, K^+). The very much higher bond strengths seen for the Mg^+ and Ca^+ singlet-state adducts, than for the corresponding triplet-state adducts, can be interpreted in terms of the influence of covalency on the metal−ligand interaction in the singlet-state adducts: if the alkaline earth ion's valence electron is of opposite spin to the unpaired electron on X, a formal single bond results. When the spins of these electrons are aligned, no such interaction is possible and the metal−ligand adduct is held together essentially solely by the ion/dipole and ion/induced dipole attraction, as is also the case for the Na^+ and K^+ adducts that lack any valence electrons on the metals. For the Al^+ adducts, metal−ligand bond formation requires the promotion of an Al valence electron from 3s to 3p (or the similarly energetically demanding task of promotion of both electrons to two sp-hybridized orbitals), and it is this requirement for electron promotion that accounts for the uniformly lower bond energies (typically by ∼100 kJ mol^{-1}) seen for Al^+ than for the corresponding singlet-state Mg^+-containing adducts.

A second trend is that, structurally, all adduct ions capable of producing a formal σ bond between M^+ and X do so (i.e., the singlet adducts of Mg^+ or Ca^+, and the Al^+-containing adducts), resulting in generally short metal−ligand separations, as well as linear $MCCH^+$ and planar $M(C_2H_3)^+$ adducts. For the "weak ionic" adducts (i.e., those of Na^+, K^+, and the triplet-state products for Mg^+ and Ca^+), σ coordination is also seen when the hydrocarbon radicals involved lack any π bonds, but competition between σ- and π-coordination occurs with the C_2H and C_2H_3 ligands, and this results in nonlinear $MCCH^+$ and nonplanar $M(C_2H_3)^+$ adducts in the MP2/6-31G* geometry optimizations used in the subsequent single-point calculations.

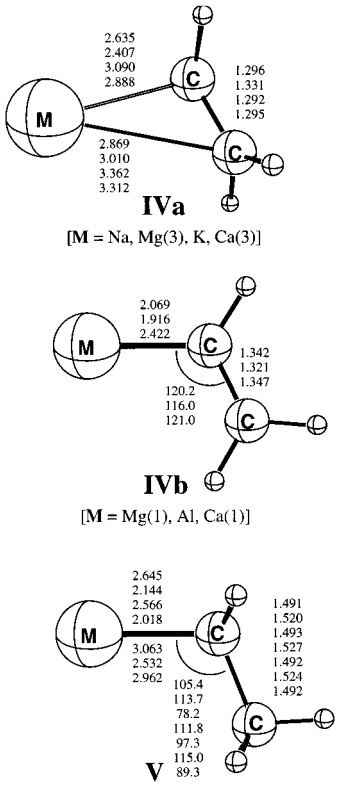

Figure 2. MP2(full)/6-31G* optimized geometries for $MC_2H_3^+$ and $MC_2H_5^+$. Bond lengths are in Ångstroms and bond angles in degrees.

The MP2/6-31G* optimized geometries of the more weakly bonded adducts, particularly $MCCH^+$ and $M(C_2H_3)^+$, merit further analysis. These adducts are rather sensitive to the level of theory employed, with B3-LYP calculations showing a tendency toward σ-coordination in these adducts. In this context, it is pertinent to note also that this preference of the B3-LYP method, for σ-coordination rather than the π-coordination indicated by MP2 optimizations, mirrors the results obtained in a previous high-level study of Mg(CN) orientation in several divalent magnesium cyanides;[101,102] QCISD(T) calculations employing large basis sets also suggest[101,102] that the apparent π-complexed structures found by MP2 optimizations are artifacts of the MP2 method rather than genuine local minima. In the divalent magnesium cyanide species, orientation of the cyanide ligand with respect to the metal atom is extremely sensitive to the level of theory employed, a phenomenon also found in the monovalent metal cyanides Na(CN),[103−106] K(CN),[103,107] and Mg(CN).[106,108] In all such species, very large changes in ligand orientation with respect to the metal atom or ion are generally associated with only minor changes to the metal−ligand bond strength, and accordingly the genuine global minimum structure can be very difficult to ascertain. The geometries obtained for $MCCH^+$ and $MC_2H_3^+$ (M = Na, K, Mg (triplet adduct) and Ca (triplet adduct)) should therefore be treated with some caution: even discounting the influence of spin contamination, these geometries are likely not to be particularly well-characterized at the MP2/6-31G* level of theory.

Tables 3 and 4 address the fluxionality seen for optimized geometries, in two respects. Table 3, which focuses on the

TABLE 2: Calculated Metal−Ligand Bond Energies

	binding energy/kJ mol^{-1} [a]						
species	Na^+	Mg^+ ($^1MX^+$)	Mg^+ ($^3MX^+$)	Al^+	K^+	Ca^+ ($^1MX^+$)	Ca^+ ($^3MX^+$)
H	4.2	196.3	0.7	59.2 (59.1)	1.9	195.6	0.1
CH_3	31.8 (31.9)	201.3	24.8 (25.0)	94.7 (94.8)	19.8 (20.0)	176.0	19.1
C_2H	44.8 (45.4)	351.9	70.3 (71.7)	227.5 (229.0)	29.1 (29.5)	396.1	78.2 (80.0)
C_2H_3	52.0 (53.3)	226.5	71.9 (73.7)	126.2 (127.6)	34.5 (35.5)	216.0	47.1 (48.5)
C_2H_5	46.5 (46.6)	195.3	54.9 (55.4)	99.5 (99.6)	30.9 (31.0)	154.1	40.5 (40.9)

[a] Metal−ligand bond energy (at 0 K), obtained via the CPd-G2thaw (for M = Na, Mg, and Al) or CP-G2 (M = K, Ca) method. The value in parentheses is the corresponding value obtained using approximate projected MP2 and MP4 energies throughout in place of unrestricted MP*n* values; this parameter is only shown when it differs measurably from the CPd-G2thaw or CP-G2 value.

TABLE 3: $MCCH^+$ (M = Na, K, Ca) Optimized Geometry Structural Dependence on Level of Theory

species	method	r_{MC}[a]	r_{CC}[a]	$\angle_{MCC}$[b]	r_{CH}[a]	$\angle_{CCH}$[b]	$\angle_{MCCH}$[b]
$NaCCH^+$	HF/6-31G*	2.766	1.215	79.0	1.063	173.5	180
	MP2(thaw)/6-31G*	2.645	1.187	86.4	1.072	179.4	
	MP3(thaw)/6-31G*	2.903	1.203	160.4	1.071	175.7	
	B3-LYP/6-31G*	2.414	1.274	166.4	1.077	172.5	180
	MP2(thaw)/6-311+G**	2.658	1.184	86.2	1.070	179.5	
	B3-LYP/6-311+G**	2.433	1.271	180	1.075	180.0	
	B3-LYP/dB4G	2.417	1.265	166.4	1.073	172.8	180
$KCCH^+$	HF/6-31G*	3.275	1.216	82.9	1.062	174.1	180
	MP2(thaw)/6-31G*	3.110	1.185	89.6	1.070	179.9	
	MP3(thaw)/6-31G*	3.119	1.187	88.4	1.070	179.7	
	B3-LYP/6-31G*	2.871	1.280	180	1.077	180.0	
	MP2(thaw)/6-311+G**	3.118	1.182	89.3	1.068	179.7	
	B3-LYP/6-311+G**	2.876	1.274	180	1.074	180.0	
	B3-LYP/6-311+G(3df,2p)	2.867	1.270	180	1.073	180.0	
$^1CaCCH^+$	HF/6-31G*	2.324	1.206	180	1.060	180	
	MP2(thaw)/6-31G*	2.314	1.239	180	1.070	180	
	MP3(thaw)/6-31G*	2.316	1.225	180	1.070	180	
	B3-LYP/6-31G*	2.300	1.225	180	1.071	180	
	MP2(thaw)/6-311+G**	2.222	1.240	180	1.070	180	
	B3-LYP/6-311+G**	2.188	1.222	180	1.068	180	
	B3-LYP/6-311+G(3df,2p)	2.176	1.218	180	1.067	180	

[a] Bond length, in Ångstroms. The value r_{MC} is always the distance between M and the terminal C of the CCH ligand. [b] Bond angle, or dihedral angle, in degrees. In structures in which one or other bond angles exceeds 175°, the dihedral angle is not well characterized and is hence not given.

TABLE 4: Dependence of $M^+−X$ Bond Energy upon Choice of Optimized Geometry, for Selected Species

	opt = MP2/6-31G*			opt = B3-LYP/dB4G	
species	r(M−X)[a]	CPd-G2thaw[b]	CPd-G2thaw(QCI)[c]	r(M−X)[a]	CPd-G2thaw[b]
$NaCCH^+$	2.65	44.8 (45.4)	46.1	2.42	62.8
$^1MgCCH^+$	1.95	351.9	351.5	1.93	346.9
$^3MgCCH^+$	2.49	70.3 (71.7)	72.2	2.29	
$AlCCH^+$	1.84	227.5 (229.0)	230.3	1.84	225.4
$KCCH^+$	3.11	29.1 (29.5)	29.5	2.87	34.3
$^1CaCCH^+$	2.31	396.1	396.0	2.18	395.9
$^3CaCCH^+$	2.71	78.2 (80.0)	79.5	2.58	72.1
$NaC_2H_3^+$	2.64	52.0 (53.3)	53.8	2.57	55.1
$^1MgC_2H_3^+$	2.07	226.5	226.8	2.06	225.8
$^3MgC_2H_3^+$	2.41	71.9 (73.7)	72.9	2.39	73.9
$AlC_2H_3^+$	1.92	126.2 (127.6)	128.8	1.97	128.1
$KC_2H_3^+$	3.09	34.5 (35.5)	35.5	3.02	36.0
$^1CaC_2H_3^+$	2.42	216.0	216.3	2.19	237.0
$^3CaC_2H_3^+$	2.88	47.1 (48.5)	48.4	2.70	46.6
$^1CaH^+$	2.04	195.6		1.89	199.4
$^1CaCH_3^+$	2.47	176.0		2.26	180.1
$^1CaC_2H_5^+$	2.53	154.1		2.22	159.5

[a] Metal−ligand bond distance, in Ångstroms, for the optimized geometry at the indicated level of theory. [b] Metal−ligand bond strength, in kJ mol^{-1}, from application of the CPd-G2thaw methodology to the indicated optimized geometry. [c] Metal−ligand bond strength, in kJ mol^{-1}, from a CPd-G2thaw(QCI) calculation, in which all single-point calculations (including those used to estimate BSSE) are at the QCISD(T)thaw/dB4G level of theory.

dependence of optimized geometry on level of theory for $NaCCH^+$, $KCCH^+$, and $^1CaCCH^+$, reveals that, for the weakly bound alkali-metal-ion complexes, the MP2 calculations favor π-complexation while B3-LYP calculations deliver σ-coordinated geometries as discussed above: there is very little apparent dependence on the basis set size. In contrast, the major influence seen in the $^1CaCCH^+$ geometries is of basis set size rather than method of electron correlation treatment: all of the calculations employing the 6-31G* basis set indicate a Ca−C separation of 2.3 Å or greater, while the calculations using the 6-311G basis set with additional polarization and diffuse functions all yield Ca−C bond lengths at least 0.1 Å shorter. This particular sensitivity of the calcium adduct-ion geometries to basis set size echoes the finding[109] that optimized geometries for CaO, CaF,

CaH, and CaOH obtained with the 6-311G basis variously augmented with polarization functions show much better agreement with experiment than do the results of calculations employing atomic natural orbital (ANO) basis sets of similar size. It has been argued[109] that the difference in performance between these families of basis sets relates to the choice of exponents used for the d functions in these calculations. Severe sensitivity to basis set size and d exponent value has elsewhere been noted for CaF_2,[110] which has not, however, been well-characterized experimentally, and for the various Ca-containing species used in the development of G2 theory for calcium.[69] In view of these results, we have performed calculations using the CPd-G2thaw methodology, with B3-LYP geometries optimized using the largest basis set (dB4G for Na, Mg, and Al, 6-311+G(3df,2p) for other atoms), for the C_2H-, C_2H_3-, and singlet Ca-containing adducts, so as to investigate the dependence of binding energy on the level of theory used in geometry optimization, and results of such calculations are given in Table 4. Discrepancies between the CPd-G2thaw methodology binding energies, calculated using the MP2/6-31G* and B3-LYP/dB4G optimized geometries, exceed 10 kJ mol^{-1} for $NaCCH^+$ and $^1CaC_2H_3^+$: in both instances it is the B3-LYP calculation, employing a large basis set, that delivers the larger value, and we therefore conclude that the B3-LYP/dB4G geometry lies closer to the true global minimum in these cases. Several other discrepancies between 5 and 10 kJ mol^{-1} are also found, and for these systems also it is usually (but not always) the B3-LYP/dB4G geometry that yields the larger binding energy. It is notable, however, that despite the major differences in Ca−ligand bond lengths obtained from MP2/6-31G* and B3-LYP/dB4G optimizations, the binding energy discrepancies for most of the Ca-containing adduct ions are generally only minor. Table 4 also shows that the agreement between CPd-G2thaw and CPd-G2thaw(QCI) calculations, where the latter method involves calculation at the QCISD(T)thaw/dB4G level of theory in all single-point steps, is excellent, particularly when correction for spin contamination in the MP2 and MP4 calculations has been effected by approximate spin projection.

One further detailed analysis of binding energy calculations, for the Al^+-containing adduct ions, is presented in Table 5. The results in this table allow us to discern the relative influence of several factors in the single-point calculations used to obtain binding energies. For example, comparison of G2 and G2thaw values reveals the sensitivity of calculated values to the correlation space (i.e., are Al 2s and 2p orbitals treated for electron correlation, as in G2thaw, or not, as in G2?), while comparison of the G2thaw and d-G2thaw results is an indicator of the influence of aluminum basis set decontraction (in the d-G2thaw values) versus use of the standard Al basis sets (in G2thaw). The most rigorous calculations reported in Table 5 are the CPd-G2full(QCI) values, which feature correction for BSSE, correlation of all electrons, and a partially decontracted Al basis set so as to better treat the contribution of aluminum inner-valence electrons to the Al−ligand bond; these calculations also involve only QCISD(T) single-point calculations (which the G2-type methods are designed to emulate, in accordance with the so-called "additivity assumption" of G2 theory and its variants) and hence should be moderately insensitive to problems arising from spin contamination.

It is apparent from the values in Table 5 that correction for basis set superposition error has only a modest effect for AlH^+, while reducing the binding energy of the Al^+/hydrocarbon radical adducts by between 4 and 5 kJ mol^{-1} (compare, for example, the d-G2thaw(QCI) and CPd-G2thaw(QCI) values).

TABLE 5: Dependence of Al^+−X Bond Energy on Level of Theory

method[a]	AlH^+ [b]	$AlCH_3^+$ [b]	$AlCCH^+$ [b]	$AlC_2H_3^+$ [b]	$AlC_2H_5^+$ [b]
G2	67.2	103.7	240.8	136.5	107.4
G2(P)[c]	67.2	103.9	242.3	137.6	107.2
CP-G2[d]	66.8	100.3	237.1	132.7	103.5
CP-G2(P)[c,d]	66.7	100.4	238.5	133.7	103.3
CBS-Q	70.8	107.2	245.2	139.7	110.9
CBS-RAD	70.9	109.2	243.8	141.1	110.9
G3	65.1	102.3	238.6	135.6	108.0
CP-G3[d]	63.6	95.7	229.2	127.1	100.4
G2thaw[e]	61.8	101.2	235.8	133.7	106.5
CP-G2thaw[d,e]	60.2	95.4	228.6	126.0	99.9
d−G2thaw[e,f]	60.1	99.3	232.8	131.4	104.7
d−G2thaw(P)[c,e,f]	60.1	99.4	234.3	132.8	104.8
d−G2thaw(QCI)[e,f,g]	61.9	100.5	235.2	133.7	105.8
d−G2full(QCI)[f,g,h]	62.6	101.5	236.6		
CPd-G2thaw[d,e,f]	59.2	94.7	227.5	126.2	99.5
CPd-G2thaw(P)[c,d,e,f]	59.1	94.8	229.0	127.6	99.6
CPd-G2thaw(QCI)[d,e,f,g]	61.1	96.2	230.3	128.8	100.9
CPd-G2full(QCI)[d,f,g,h]	61.7	96.9	230.8		

[a] Computational method. The "standard" methods G2, G3, CBS-Q, and CBS-RAD are as defined in the literature. Variants of the Gaussian model chemistries are modified as indicated. [b] Bond energy, in kJ mol^{-1}, at 0 K and incorporating a scaled (0.8929) HF/6-31G* correction for zero-point vibrational energy. [c] "(P)" suffix denotes use of spin-projected MP2 and MP4 energies, rather than unrestricted Moller−Plesset values, in single-point calculations. [d] "CP" prefix indicates incorporation of a geometry-corrected counterpoise correction for BSSE, calculated at the highest level of correlation [i.e., MP2, or, in G2(QCI)-type calculations, QCISD(T)] used in the largest-basis-set single-point calculation. [e] "Thaw" suffix denotes inclusion of the Al 2s and 2p orbitals in the correlation space in all single-point calculations. [f] "d-" prefix indicates partial decontraction of the Al 6-311+G(3df,2p) basis set, as described in the text. [g] "(QCI)" suffix indicates a calculation combining QCISD(T) and the largest G2 or d-G2 basis set (B4G or d-B4G, see text) as the only level of theory employed in single-point calculations. [h] "Full" suffix describes correlation of all electrons in the constituent single-point calculations.

Neglect of BSSE thus leads to apparent overestimation in the calculated Al^+/ligand binding energies. Comparison of CPd-G2thaw and CPd-G2thaw(QCI) values shows that the additivity assumption does not exactly hold true: the former method underestimates the latter values by between 1.4 and 3 kJ mol^{-1}, with the greatest discrepancies seen for the most significantly spin contaminated Al^+ adducts, those with C_2H and C_2H_3. Correction for spin contamination, by use of projected Moller−Plesset energies in the CPd-G2thaw(P) method, yields a reduced discrepancy against CPd-G2thaw(QCI) for the C_2H and C_2H_3 adducts but is otherwise ineffective in improving the additivity of the CPd-G2thaw method. Use of a standard 6-311+G(3df) Al basis set, as in CP-G2thaw, yields values that are close to those obtained using a partially decontracted Al basis set, as in CPd-G2thaw: the largest deviation between these two methods is 1.1 kJ mol^{-1}, for $AlCCH^+$. Note, however, that the influence of basis set decontraction is much larger if the values being compared are not corrected for BSSE (as in, for example, G2thaw and dG2thaw): here the values obtained using a partially decontracted Al basis set are uniformly significantly lower, by up to 3 kJ mol^{-1}. Correction for BSSE is thus able to rectify most of the apparent overestimation associated with use of the standard 6-311+G(3df) Al basis set. We can also examine the influence of correlation space, most conveniently done by comparing G2 and G2thaw results: the G2 values (employing a standard "frozen core" and thereby neglecting correlation of the Al 2s and 2p orbitals) are uniformly higher than the G2thaw results, by ≥5 kJ mol^{-1} in the cases of AlH^+ and $AlCCH^+$. Even larger discrepancies between "frozen core" and "thawed" binding energies are seen when BSSE corrections are applied,

as in CP-G2 and CP-G2thaw: the disagreement between these two methods, for $AlCCH^+$, reaches 8.5 kJ mol^{-1}. We conclude that counterpoise correction for BSSE is not adequate to redress the binding energy overestimation associated with use of a standard frozen core for Al. In contrast, comparison of the d-G2thaw(QCI) and d-G2full(QCI) results shows that the effect of further expansion of the correlation space, from the "thawed" space to full correlation, is minor, particularly after correction for BSSE; the close agreement between the CPd-G2thaw(QCI) and CPd-G2full(QCI) results provides additional justification for use of a "thawed" correlation space in metal cation affinity calculations.

Methods other than G2 variants also feature in Table 5. The CBS-Q and CBS-RAD results are consistently about 10 kJ mol^{-1} higher than our most computationally expensive (CPd-G2thaw(QCI)) values. These complete basis set methods feature a standard frozen core for Al and are not corrected for BSSE, nor can such a correction be readily applied: it appears that the core size and BSSE effects, which arguably have the greatest influence on calculated binding energy of all the various effects considered in our comparison of G2-variant results in Table 5, are largely responsible for the very poor agreement between CBS-Q and the CPd-G2thaw(QCI) values. Improved treatment of spin contamination, as in CBS-RAD, cannot in this case significantly diminish the level of discrepancy versus CPd-G2thaw(QCI). Better agreement is seen between G3 and CPd-G2thaw(QCI), and this is further improved when a counterpoise correction is applied to the G3 values (as in CP-G3). The G3 method features correlation of all electrons in its largest basis set single point calculation, and of the "standard" model chemistry methods (G2, CBS-Q, and G3) it thus appears the most reliable for purposes of obtaining metal−ligand binding energies, though a BSSE correction appears necessary as other researchers have already noted for Na^+-containing ions.[89]

In summary, the results in Table 5 indicate that

(a) inclusion of metal-ion 2s and 2p electron correlation is an important influence on the binding energy for Al-containing ions, as has already been shown elsewhere for Na-containing ions,[83,84,86−88] and we infer that this is also the case for Mg-containing ions;

(b) correction for BSSE is also important and can apparently compensate for deficiencies in the Al basis set, but not for errors arising from an inappropriate correlation space or from a neglect of spin contamination;

(c) partial decontraction of the Al basis set has only a small influence on the calculated binding energy, particularly when a BSSE correction is applied, though for Na-containing species[90] and, we suspect, for Mg-containing ions also, metal orbital basis set decontraction has a larger effect;

(d) correction for spin contamination, by projection of the Moller−Plesset single-point energies, does not have a large influence on binding energies of the Al-containing adduct ions (which are the most heavily spin contaminated doublet ions in the present study); neglect of this effect in calculations on main-group-metal-containing adduct ions thus appears less significant as a potential source of error than do the factors noted in (a) and (b) above.

3.2. Comparison with Previous Results. High-level calculations have been reported previously only for MH^+ (M = Na, Mg, Al, K, and Ca), MCH_3^+ (M = Na, Mg, Al), and $MgCCH^+$, while an experimental determination of the thermochemistry of these species has been performed only for MgH^+. A curious dichotomy exists in the experimental results for MgH^+: spectroscopic studies yield a bond dissociation energy (2.080 eV)[111] in very good agreement with our CPd-G2thaw value of 2.034 eV, while the sole reported measurement of the proton affinity of Mg, PA(Mg) [$=D_0(Mg-H^+)$] = 819.6 kJ mol^{-1},[112] is almost 60 kJ mol^{-1} higher than our calculated zero *K* value of 761.9 kJ mol^{-1} for this parameter. The experimental measurement of PA(Mg), reported in 1977 and still listed as the recommended value in the NIST web book,[113,114] derives from the inferred occurrence of exothermic proton transfer (PT) from $t\text{-}C_4H_9^+$ ($PA((CH_3)_2CCH_2)$ = 802.1 kJ mol^{-1}) and apparently endothermic PT from NH_4^+ ($PA(NH_3)$ = 853.6 kJ mol^{-1}). This experimental PA(Mg) value is at variance not only with our calculated value, but directly with the results of a CEPA (coupled electron pair approximation) calculation of this parameter,[37] and indirectly (since the ionization energies of Mg and H are both well established) with a large body of calculated $D(Mg^+-H)$ values,[42,44−48,51−53] all of which show good to excellent agreement with our CP-dG2thaw value of $D(Mg^+-H)$. Furthermore, the experimental PA(Mg) value is also in direct conflict with the spectroscopic determination of the Mg^+-H bond strength.[111] We suggest that the reactions leading to MgH^+ in the study of Po and Porter[112] may have been incorrectly assigned. Note also that the subsequent determination of PA(Mg_2) by those authors[115] is also expected to be in error, since their value of this parameter[115] was based on the PA(Mg) value.[112] We have performed additional calculations, at the CPd-G2thaw(QCI) level of theory (for B3-LYP/dB4G optimized geometries), on Mg_2 and Mg_2H^+ with which to assess the experimental value of PA(Mg_2). Curiously, while our PA(Mg) value is significantly lower than the experimental PA(Mg), our calculated PA(Mg_2) = 981.5 kJ mol^{-1} is much higher than Po and Porter's laboratory result of PA(Mg_2) = 917 ± 29 kJ mol^{-1}.[115] An even more extreme discrepancy therefore exists between our calculated (221.0 kJ mol^{-1}) and the experimental (100 ± 21 kJ mol^{-1})[115] value of the $Mg-MgH^+$ dissociation energy. While the source of this discrepancy is unclear, we note that the authors of the experimental study[115] surmised that Mg_2H^+ was arising through the equilibrium

$$MgH^+(g) + Mg(s) \leftrightarrow Mg_2H^+(g) \qquad (4)$$

that is, by ion sputtering of the solid magnesium surface in their apparatus. If instead the Mg_2H^+ was arising through a purely gas-phase process such as

$$MgH^+(g) + Mg(g) \leftrightarrow Mg_2H^+(g) \qquad (5)$$

then the experimental (gas-phase) value of $D_0(Mg-MgH^+)$ would be elevated by $\Delta H°_f(Mg(g)) - \Delta H°_f(Mg(s))$, to yield a result much closer to the calculated quantity. This would not, however, improve the agreement between calculated and experimental proton affinities of the magnesium dimer. We conclude by urging an experimental reevaluation of the thermochemistry surrounding MgH^+ and Mg_2H^+.

Comparison with the limited set of previously reported calculated thermochemical values for the MH^+ and MCH_3^+ species (see Table 6) indicates that the agreement between values determined at different levels of theory is generally very good, with the largest absolute discrepancy being 0.21 eV for the Olson and Liu value of $D(Mg^+-H)$.[45] The value of the Na^+-H bond strength obtained by Rosmus et al.[37] is, at 0.12 eV, almost three times as high as the set of tightly clustered values in the range 0.041−0.053 eV,[39−41,43] into which our CP-dG2thaw value of 0.044 eV fits comfortably: factors influencing the apparently erroneously high value of Rosmus et al.[37] have already been discussed by Liu et al.[41] elsewhere.

TABLE 6: Comparison of Calculated (CP-dG2thaw) and Literature Values for M^+-H Bond Strengths and Metal Atom Proton and Methyl Cation Affinities

M	$D_0(M^+-H)$/ eV [a]	lit. D_0 [b]	PA/ kJ mol^{-1} [c]	lit. PA [d]	MCA/ kJ mol^{-1} [e]
Na	0.044	0.041 ± 0.025 [f,g] 0.12 ± 0.05 [h] 0.041 [g,i] 0.044 ± 0.01 [g,j] 0.053 eV [g,k]	825.5	828 [h]	484.5
Mg	2.034	2.00 [h] 1.82 [g,l] 2.08 [g,n] 1.853 [o] 2.080 [p] 1.99 [q]	761.9	767 [h] 819.6 [m]	398.1
Al	0.614	0.67 [h]	802.1	799 [h]	468.9
K	0.020	0.022 [g,i]	902.5		551.5
Ca	2.027	1.934 [r] 1.922 [g,n] 2.070 [s] 1.835 [o]	912.1		522.8

[a] Bond strength, obtained in the present work [b] Literature value of the M^+-H bond strength, in eV. Experimental values are indicated in bold text. [c] Metal atom proton affinity (corresponding to the $M-H^+$ bond dissociation energy) at 0 K, obtained in the present work [d] Literature proton affinity value, in kJ mol^{-1}. Experimental values are indicated in bold text. [e] Metal atom methyl cation affinity (corresponding to the $M-CH_3^+$ bond dissociation energy) at 0 K, obtained in the present work [f] CI calculation, ref 40. [g] Obtained from the published D_e value, with correction for zero-point vibrational energy using the B3-LYP/dB4G calculated harmonic frequency. [h] PNO-CI calculation, ref 37. [i] HF calculation, ref 39. [j] CI calculation, ref 41. [k] Model potential calculation, ref 43. [l] CI calculation, ref 45. [m] Result of a high-temperature ion−molecule laboratory study, ref 112, subsequently adjusted (refs 113, 114) in line with new reference base PA values. [n] Pseudopotential calculation, ref 47. [o] MP4 calculation, ref 50. [p] Spectroscopic determination, ref 111. [q] Complete basis set extrapolation from RCCSD(T) calculation, ref 53. [r] CI calculation, ref 66. [s] Reference 64.

Finally, our calculation on $MgCCH^+$ yields a result in good agreement with the high-level study of Woon[53] on this species.

3.3. Implications for Metal-Ion Reactivity in Gaseous Environments. Inflow of exogenous material, viz., meteoritic ablation in the upper atmospheres of Jupiter,[7,15] Saturn,[13] Titan,[8,11,14] and Neptune,[9,10] as well as cometary bombardment[12,15] and infall of metal ions from Io's plasma torus into Jupiter's atmosphere,[7] have been considered as viable sources of sporadic-E ion/electron layer formation within these reducing atmospheres.

One important finding of the present study concerns the reactivity of Mg^+ with C_2H_3 and C_2H_5. Both of these radicals are expected to be present at trace concentrations (peak mixing ratio $\sim 10^{-10}$)[116] in Jupiter's upper atmosphere, within the altitude range appropriate for sporadic-E layer formation via meteoritic ablation.[15] While a detailed assessment of the association chemistry must await determination of the relevant association rate coefficients, it appears that the bimolecular processes

$$Mg^+ + C_2H_3 \rightarrow MgH^+ + C_2H_2 \qquad (6)$$

and

$$Mg^+ + C_2H_5 \rightarrow MgH^+ + C_2H_4 \qquad (7)$$

are substantially exothermic (on the singlet state potential energy surface) and are presumably not constrained by activation barriers. These processes will therefore compete with association as loss processes for Mg^+ with these radicals. If we assume a typical rate coefficient of $\sim 3 \times 10^{-10}$ for these reactions (i.e., approximately 25% of the expected collision rate coefficient, reflecting the statistical weight of $^1/_4$ relevant to two doublet reactants accessing a singlet-state potential enerrgy surface), then the processes (6) and (7) will outweigh the radiative recombination of Mg^+ with e by at least 1 order of magnitude in the altitude range assigned[15] to the putative sporadic-E layer. Analogous reactions with larger hydrocarbon radicals (some having comparable Jovian mixing ratios to those of C_2H_3 and C_2H_5),[116] not explicitly characterized here, are almost certainly viable also, as are exothermic charge-transfer reactions of Mg^+ with secondary alkyl radicals such as $(CH_3)_2CH$ and CH_3CH_2-$CHCH_3$, and even the abstraction of smaller alkyl radicals such as CH_3 and C_2H_3 from yet larger radicals. The occurrence of such reactions, which are not included in the Jovian meteoritic model of Kim et al.,[15] thus calls into question their conclusion that Mg^+ is the predominant ion resulting from meteoritic ablation in such atmospheres. Rather, we would infer that the loss processes for Mg^+ (and Ca^+ and, to a lesser extent, Al^+) are probably much more efficient than the loss processes for Na^+ and K^+, since the latter ions invariably have lower binding energies to ligands than do their group II and group III counterparts and are consequently expected to have generally lower rate coefficients for adduct formation. While this hypothesis remains to be rigorously tested by more detailed chemical models, it nevertheless appears likely that the predominant metal ions produced by meteoritic ablation in outer planetary atomspheres are the long-lived alkali metal ions Na^+ and K^+; note that these are also the main metal ions associated with sporadic-E layer formation in Earth's upper atmosphere,[4−6] as well as being the main metallic components of the tenuous atmosphere associated with Jupiter's satellite Io.[117]

4. Conclusions

Our high-level calculations on the adducts of main group metal cations with small hydrocarbon radicals reveal a very marked gradation in M^+-ligand bond strengths for such species, with group II cations exhibiting much stronger bonds than group I cations to these radicals. This trend can very satisfactorily be accounted for by the much greater covalent character expected for the Mg^+-ligand bond, for example, than for the corresponding Na^+-ligand bond, while the intermediate bond strengths seen for Al^+/radical adducts is consistent with formation of a significantly covalent bond at the expense of Al^+ electronic promotion from 3s to 3p. This very marked disparity between alkali metal and alkaline earth cation bond strengths is expected to have major implications for the relative persistence of such metal ions in reducing atmospheres, and we suggest that Na^+ rather than Mg^+ is more likely to be the major long-lived metal ion associated with sporadic E-type activity in the atmospheres of the outer planets.

Comparison of our calculated results with the existing literature values shows generally good agreement, although we recommend that the laboratory thermochemistry of protonation of Mg and of Mg_2 should be revisited.

References and Notes

(1) Ferguson, E. E.; Fehsenfeld, F. C. *J. Geophys. Res.* **1968**, *73*, 6215.
(2) Plane, J. M. C. *Int. Rev. Phys. Chem.* **1991**, *10*, 55.
(3) McNeil, W. J.; Lai, S. T.; Murad, E. *J. Geophys. Res.* **1996**, *101*, 5251.
(4) Cox, R. M.; Plane, J. M. C. *J. Chem. Soc., Faraday Trans.* **1997**, *93*, 2619.
(5) Cox, R. M.; Plane, J. M. C. *J. Geophys. Res.* **1998**, *103*, 6349.

(6) Heinselman, C. J. *J. Geophys. Res.* **2000**, *105*, 12181.
(7) Atreya, S. K. *Adv. Space Res.* **1984**, *4*, 31.
(8) Ip, W. H. *Nature* **1991**, *345*, 511.
(9) Moses, J. I. *Icarus* **1992**, *99*, 368.
(10) Lyons, J. R. *Science* **1995**, *267*, 648.
(11) English, M. A.; Lara, L. M.; Lorenz, R. D.; Ratcliff, P. R.; Rodrigo, R. *Adv. Space Res.* **1995**, *17*, 157.
(12) Moses, J. I. *J. Geophys. Res.* **1997**, *102*, 21619.
(13) Moses, J. I.; Bass, S. F. *J. Geophys. Res.* **2000**, *105*, 7013.
(14) Molina-Cuberos, G. J.; Lammer, H.; Stumptner, W.; Schwingenschuh, K.; Rucker, H. O.; Lopez-Moreno, J. J.; Rodrigo, R.; Tokano, T. *Planet Space Sci.* **2001**, *49*, 143.
(15) Kim, Y. H.; Pesnell, W. D.; Grebowsky, J. M.; Fox, J. L. *Icarus* **2001**, *150*, 261.
(16) Herbst, E.; Leung, C. M. *Mon. Not. R. Astron. Soc.* **1986**, *222*, 689.
(17) Millar, T. J.; Rawlings, J. M. C.; Bennett, A.; Brown, P. D.; Charnley, S. B. *Astron. Astrophys. Suppl. Ser.* **1991**, *87*, 585.
(18) Millar, T. J. In *Galactic and Extragalactic Infrared Spectroscopy*; Kessler, M. F., Phillips, J. P., Ed.; ESA SP-192; Reidel: Dordrecht, The Netherlands, 1984; p 33.
(19) Graedel, T. E.; Langer, W. D.; Frerking, M. A. *Astrophys. J. Suppl. Ser.* **1982**, *48*, 321.
(20) Petrie, S. *Mon. Not. R. Astron. Soc.* **1996**, *282*, 807.
(21) Petrie, S. *Mon. Not. R. Astron. Soc.* **1999**, *302*, 482.
(22) Petrie, S.; Dunbar, R. C. *J. Phys. Chem. A* **2000**, *104*, 4480.
(23) Dunbar, R. C.; Petrie, S. *Astrophys. J.* **2002**, *564*, 792.
(24) Ziurys, L. M.; Apponi, A. J.; Guelin, M.; Cernicharo, J. *Astrophys. J.* **1995**, *445*, L47.
(25) Kawaguchi, K.; Kagi, E.; Hirano, T.; Takano, S.; Saito, S. *Astrophys. J.* **1993**, *406*, L39.
(26) Ziurys, L. M.; Savage, C.; Highberger, J. L.; Apponi, A. J.; Guelin, M.; Cernicharo, J. *Astrophys. J.* **2002**, *564*, L45.
(27) Guelin, M.; Muller, S.; Cernicharo, J.; Apponi, A. J.; McCarthy, M. C.; Gottlieb, C. A.; Thaddeus, P. *Astron. Astrophys.* **2000**, *363*, L9.
(28) Atreya, S. K. *Adv. Space Res.* **1987**, *7*, 79.
(29) Romani, P. N.; Atreya, S. K. *Icarus* **1988**, *74*, 424.
(30) Kim, Y. H.; Fox, J. L. *Icarus* **1994**, *112*, 310.
(31) Bezard, B.; Feuchtgruber, H.; Moses, J. I.; Encrenaz, T. *Astron. Astrophys.* **1998**, *334*, L41.
(32) Moses, J. I.; Bezard, B.; Lellouch, E.; Gladstone, G. R.; Feuchtgruber, H.; Allen, M. *Icarus* **2000**, *143*, 244.
(33) Yung, Y. L.; Allen, M.; Pinto, J. P. *Astrophys. J. Suppl. Ser.* **1984**, *55*, 465.
(34) Toublanc, D.; Parisot, J. P.; Brillet, J.; Gautier, D.; Raulin, F.; McKay, C. P. *Icarus* **1995**, *113*, 2.
(35) Lara, L. M.; Lellouch, F.; Lopez-Moreno, J. J.; Rodrigo, R. *J. Geophys. Res. E* **1996**, *101*, 23261.
(36) Banaszkiewicz, M.; Lara, L. M.; Rodrigo, R.; Lopez-Moreno, J. J.; Molina-Cuberos, G. J. *Icarus* **2000**, *147*, 386.
(37) Rosmus, P.; Meyer, W. *J. Chem. Phys.* **1977**, *66*, 13.
(38) Valance, A. *Chem. Phys. Lett.* **1978**, *56*, 289.
(39) Melius, C. F.; Numrich, R. W.; Truhlar, D. G. *J. Phys. Chem.* **1979**, *83*, 1221.
(40) Olson, R. E.; Saxon, R. P.; Liu, B. *J. Phys. B* **1980**, *13*, 297.
(41) Liu, B.; Olson, R. E.; Saxon, R. P. *J. Chem. Phys.* **1981**, *74*, 4216.
(42) Curtiss, L. A.; Pople, J. A. *J. Phys. Chem.* **1988**, *92*, 894.
(43) Patil, S. H.; Tang, K. T. *J. Chem. Phys.* **2000**, *113*, 676.
(44) Numrich, R. W.; Truhlar, D. G. *J. Phys. Chem.* **1975**, *79*, 2745.
(45) Olson, R. E.; Liu, B. *Phys. Rev. A* **1979**, *20*, 1366.
(46) Pyykko, P. *J. Chem. Soc., Faraday Trans. 2* **1979**, *75*, 1256.
(47) Fuentealba, P.; Reyes, O. *Mol. Phys.* **1987**, *62*, 1291.
(48) Walther, P.; Gruendler, W. *Z. Chem.* **1989**, *29*, 221.
(49) Garcia-Madronal, J. C.; Mo, O.; Cooper, I. L.; Dickinson, A. S. *THEOCHEM* **1992**, *92*, 63.
(50) Canuto, S.; Castro, M. A.; Sinha, K. *Phys. Rev. A* **1993**, *48*, 2461.
(51) Gardner, P. J.; Preston, S. R.; Siertsema, R.; Steele, D. R. *J. Comput. Chem.* **1993**, *14*, 1523.
(52) Petrie, S. *J. Chem. Soc., Faraday Trans.* **1996**, *92*, 1135.
(53) Woon, D. E. *Astrophys. J.* **1996**, *456*, 602.
(54) Sabelli, N. H.; Kantor, M.; Benedek, R.; Gilbert, T. L. *J. Chem. Phys.* **1978**, *68*, 2767.
(55) Trivedi, H. P.; Richards, W. G. *J. Chem. Phys.* **1980**, *72*, 3438.
(56) Guest, M. F.; Hirst, D. M. *Chem. Phys. Lett.* **1981**, *84*, 167.
(57) Klein, R.; Rosmus, P.; Werner, H. J. *J. Chem. Phys.* **1982**, *77*, 3559.
(58) Cooper, D. L.; Black, J. H.; Everard, M. A. L.; Richards, W. G. *J. Chem. Phys.* **1983**, *78*, 1371.
(59) Biskupic, S.; Klein, R. *THEOCHEM* **1988**, *47*, 27.
(60) Cramer, C. J. *THEOCHEM* **1991**, *81*, 243.
(61) Rusho, J.; Nichols, J.; Simons, J. *Int. J. Quantum Chem.* **1993**, *48*, 309.
(62) Chambaud, G.; Rosmus, P.; Senent, M. L.; Palmieri, P. *Mol. Phys.* **1997**, *92*, 399.
(63) Mueller, B.; Ottinger, C. *Z. Naturforsch., A* **1998**, *43*, 1007.
(64) McFarland, R. H.; Schlachter, A. S.; Stearns, J. W.; Liu, B.; Olson, R. E. *Phys. Rev. A* **1982**, *26*, 775.
(65) Schilling, J. B.; Goddard, W. A., III.; Beauchamp, J. L. *J. Am. Chem. Soc.* **1986**, *108*, 582.
(66) Schilling, J. B.; Goddard, W. A., III.; Beauchamp, J. L. *J. Phys. Chem.* **1987**, *91*, 5616.
(67) Kaupp, M.; Schleyer, P. v. R.; Stoll, H.; Preuss, H. *J. Chem. Phys.* **1991**, *94*, 1360.
(68) Boutalib, A.; Daudey, J. P.; El Mouhtadi, M. *Chem. Phys.* **1992**, *167*, 111.
(69) Blaudeau, J.-P.; McGrath, M. P.; Curtiss, L. A.; Radom, L. *J. Chem. Phys.* **1997**, *107*, 5016.
(70) Bews, J. R.; Glidewell, C. *THEOCHEM* **1982**, *7*, 151.
(71) Clark, T. *J. Am. Chem. Soc.* **1988**, *110*, 1672.
(72) Ortiz, J. V. *J. Chem. Phys.* **1990**, *92*, 6728.
(73) Srinivas, R.; Suelzle, D.; Schwarz, H. *J. Am. Chem. Soc.* **1990**, *112*, 8334.
(74) Bauschlicher, C. W., Jr.; Partridge, H. *Chem. Phys. Lett.* **1991**, *181*, 129.
(75) Safont, V. S.; Moliner, V.; Oliva, M.; Castillo, R.; Andres, J.; Gonzalez, F.; Carda, M. *J. Org. Chem.* **1996**, *61*, 3467.
(76) Stoeckigt, D. *Chem. Phys. Lett.* **1996**, *250*, 387.
(77) Peralez, E.; Negrel, J.-C.; Goursot, A.; Chanon, M. *Main Group Metal Chem.* **1999**, *22*, 185.
(78) White, J. C.; Cave, R. J.; Davidson, E. R. *J. Am. Chem. Soc.* **1988**, *110*, 6308.
(79) Cheng, Y. C.; Chen, J.; Ding, L. N.; Wong, T. H.; Kleiber, P. D.; Liu, D.-K. *J. Chem. Phys.* **1996**, *104*, 6452.
(80) Armentrout, P. B.; Rodgers, M. T. *J. Phys. Chem. A* **2000**, *104*, 2238.
(81) Hofmann, H.; Hänsele, E.; Clark, T. *J. Comput. Chem.* **1990**, *11*, 1147.
(82) Duke, B. J.; Radom, L. *J. Chem. Phys.* **1998**, *109*, 3352.
(83) Petrie, S. *Chem. Phys. Lett.* **1998**, *283*, 181.
(84) Petrie, S. *J. Phys. Chem. A* **1998**, *102*, 6138.
(85) Bauschlicher, C. W., Jr.; Melius, C. F.; Allendorf, M. D. *J. Chem. Phys.* **1999**, *110*, 1879.
(86) Ma, N. L.; Siu, F. M.; Tsang, C. W. *Chem. Phys. Lett.* **2000**, *322*, 65.
(87) Soldán, P.; Lee, E. P. F.; Wright, T. G. *J. Chem. Soc., Faraday Trans.* **1998**, *94*, 3307.
(88) Hoyau, S.; Norrman, K.; McMahon, T. B.; Ohanessian, G. *J. Am. Chem. Soc.* **1999**, *121*, 8864.
(89) Siu, F. M.; Ma, N. L.; Tsang, C. W. *J. Chem. Phys.* **2001**, *114*, 7045.
(90) Petrie, S. *J. Phys. Chem. A* **2001**, *105*, 9931.
(91) Magnusson, E. A. Personal communication.
(92) Curtiss, L. A.; Raghavachari, K.; Trucks, G. W.; Pople, J. A. *J. Chem. Phys.* **1991**, *94*, 7221.
(93) Krishnan, R.; Binkley, J. S.; Seeger, R.; Pople, J. A. *J. Chem. Phys.* **1980**, *72*, 650.
(94) Petrie, S. *J. Mol. Struct. (THEOCHEM)* **1998**, *429*, 1.
(95) Barrientos, C.; Redondo, P.; Largo, A. *Chem. Phys. Lett.* **2000**, *320*, 481.
(96) Redondo, P.; Barrientos, C.; Largo, A. *Chem. Phys. Lett.* **2001**, *335*, 64.
(97) Barrientos, C.; Redondo, P.; Largo, A. *Chem. Phys. Lett.* **2001**, *343*, 563.
(98) Mayer, P. M.; Parkinson, C. J.; Smith, D. M.; Radom, L. *J. Chem. Phys.* **1998**, *108*, 604.
(99) There are several reasons why we have not used CBS-RAD for the other adduct ions for which spin contamination is potentially problematic. First, CBS-RAD is not defined for third-row atoms, precluding its implementation on K- and Ca-containing adducts. Second, CBS-RAD uses single-point calculations with a standard "frozen core", so that neglect of inner-valence correlation (an important consideration in calculation on alkali metal ions, in particular) may limit its reliability in calculations on Na- and Mg-containing adducts. Third, the ability of the CBS-type methods to compensate for metal/ligand basis set superposition error (BSSE) effects is not apparent, again limiting the reliability of the method particularly for Na- and Mg-containing adducts. Finally, the Al^+ adducts are in any case those that generally display the greatest increase in spin contamination upon metal/ligand complexation: for the other doublet-state adducts, the value for $\langle S^2 \rangle$ is close to the corresponding free-ligand value, suggesting that any errors arising from spin contamination in the other adducts are likely to cancel out in computation of the metal ion/ligand binding energy.
(100) Frisch, M. J.; Trucks, G. W.; Schegel, H. B.; Scuseria, G. E.; Robb, M. A.; Cheeseman, J. R.; Zakrzewski, V. G.; Montgomery, J. A., Jr.; Stratmann, R. E.; Burant, J. C.; Dapprich, S.; Millam, J. M.; Daniels, A. D.; Kudin, K. N.; Strain, M. C.; Farkas, O.; Tomasi, J.; Barone, V.; Cossi, M.; Cammi, R.; Mennucci, B.; Pomelli, C.; Adamo, C.; Clifford, S.; Ochterski, J. W.; Petersson, G. A.; Ayala, P. Y.; Cui, Q.; Morokuma, K.;

Malick, D. K.; Rabuck, A. D.; Raghavachari, K.; Foresman, J. B.; Cioslowski, J.; Ortiz, J. V.; Stefanov, B. B.; Liu, G.; Liashenko, A.; Piskorz, P.; Komaromi, I.; Gomperts, R.; Martin, R. L.; Fox, D. J.; Keith, T.; Al-Laham, M. A.; Peng, C. Y.; Nanayakkara, A.; Gonzalez, C.; Challacombe, M.; Gill, P. M. W.; Johnson, B. G.; Chen, W.; Wong, M. W.; Andres, J. L.; Head-Gordon, M.; Replogle, E. S.; Pople, J. A. Gaussian98; Gaussian, Inc.: Pittsburgh, PA, 1998.

(101) Petrie, S. *J. Phys. Chem. A* **1999**, *103*, 2107.

(102) Petrie, S. *Int. J. Quantum Chem.* **2000**, *76*, 626.

(103) Marsden, C. J. *J. Chem. Phys.* **1982**, *76*, 6451.

(104) Dorigo, A.; Schleyer, P. v. R.; Hobza, P. *J. Comput. Chem.* **1994**, *15*, 322.

(105) Spoliti, M.; Ramondo, F.; Diomedi-Camassei, F.; Bencivenni, L. *THEOCHEM* **1994**, *312*, 41.

(106) Petrie, S. *J. Phys. Chem.* **1996**, *100*, 11581.

(107) Petrie, S. *Phys. Chem. Chem. Phys.* **1999**, *1*, 2897.

(108) Barrientos, C.; Largo, A. *THEOCHEM* **1995**, *336*, 29.

(109) Wesolowski, S. S.; Valeev, E. F.; King, R. A.; Baranovski, V.; Schaefer, H. F., III. *Mol. Phys.* **2000**, *98*, 1227.

(110) Hassett, D. M.; Marsden, C. J. *J. Mol. Struct.* **1995**, *346*, 249.

(111) Herzberg, G. *Molecular Spectra and Molecular Structure, I. Spectra of Diatomic Molecules*, 2nd ed.; Van Nostrand: Princeton, NJ, 1955.

(112) Po, P. L.; Porter, R. F. *J. Am. Chem. Soc.* **1977**, *99*, 4922.

(113) Hunter, E. P.; Lias, S. G. *J. Phys. Chem. Ref. Data* **1998**, *27*, 413.

(114) Hunter, E. P.; Lias, S. G. Proton Affinity Evaluation. In *NIST Chemistry WebBook*; Linstrom, P. J., Mallard, W. G., Eds.; NIST Standard Reference Database Number 69; National Institute of Standards and Technology, Gaithersburg MD, 20899 (http://webbook.nist.gov); July 2001.

(115) Po, P. L.; Porter, R. F. *J. Phys. Chem.* **1977**, *81*, 2233.

(116) Gladstone, G. R.; Allen, M.; Yung, Y. L. *Icarus* **1996**, *119*, 1.

(117) Brown, M. E. *Icarus* **2001**, *151*, 190.